

Heteroflocculation in Binary Colloidal Suspensions: Monte Carlo Simulations

Wan Y. Shih,^{*,†,‡} Wei-Heng Shih,^{*,‡} and İlhan A. Aksay^{*,†}

Department of Chemical Engineering and Princeton Materials Institute,
Princeton University, Princeton, New Jersey 08544-5211

Department of Materials Engineering, Drexel University, Philadelphia, Pennsylvania 19104

We have examined heteroflocculation in binary colloidal suspensions by Monte Carlo simulations based on a diffusion-limited-cluster-aggregation (DLCA) model modified with finite attraction energies. The simulations were performed in two dimensions. Under heteroflocculation conditions, i.e., attraction between unlike particles and repulsion between like particles, cluster size undergoes a maximum as the concentration of the second species of particles is increased, similar to the experimental results in both binary suspensions and suspensions with adsorbing polymers. The initial increase in cluster size at low concentrations of the second species of particles is due to the mutual attraction between unlike particles. The decrease in cluster size at higher concentrations of the second species of particles is due to the repulsion between the second species of particles. The distinction between heteroflocculation and particulate depletion flocculation is discussed.

I. Introduction

MULTIPHASE compacts are often required for reaction sintering (e.g., mullite)¹ or for incorporating sintering aids (e.g., silicon nitride).²⁻⁴ In such compacts, uniform distribution of each of the constituent phases is crucial for improving the sintering of the compacts²⁻⁴ or controlling the reaction temperature.¹ Homogeneous mixing between the constituent phases can be achieved either by coating particles in a solution (e.g., heterogeneous nucleation)²⁻⁵ or through heterocoagulation of colloidal particles.⁶⁻⁹ The solution coating approach involves precipitation of one constituent phase (or more) on particles of the other phase. In the colloidal coating approach, all constituent phases are in the particulate form. Coating in this approach involves adsorbing particles of one phase onto particles of another phase. Adsorption may be achieved by electrostatic attraction between the unlike particles or by reduction of the repulsive barrier between the unlike particles. Electrostatic attraction occurs between unlike particles when they have opposite surface charges.⁶⁻⁸ For unlike particles with surface charges of the same sign, reduction of the repulsion barrier between unlike particles occurs when the size of one species of particles is much smaller than that of the other species of particles.⁹ The adsorption of one species of particles onto the other species of particles can also cause flocculation in the suspension.⁹⁻¹⁴ For example, before adsorption saturation takes place, a partially coated particle may form a cluster with either

another partially coated particle or an uncoated particle by sharing one or more of the adsorbing particles. That is, clustering of one species of particles is mediated by the adsorbing species of particles. We refer to this phenomenon as heteroflocculation. Heteroflocculation is also termed bridging flocculation¹⁰⁻¹² in the colloids literature as the adsorbed second species of particles act as bridges between the first species of particles. It is also referred to as mutual flocculation¹³ or mutual coagulation¹⁴ in the earlier coagulation studies. Heteroflocculation can lead to intimate mixing between different species of particles and thus play a useful role in achieving homogeneity in sintered samples. However, heteroflocculation could also have a negative effect due to the formation of large clusters in the suspension that can degrade both the packing density and the density uniformity of a compact. In order to optimize the packing density as well as the density uniformity of the green compacts, it is necessary to understand how clustering takes place as the concentration of each species of particles varies.

Here, we report the results of our computer simulations on heteroflocculation in binary colloidal suspensions. Unlike the previous theoretical studies,^{10,14} the focus of the present simulations is the size and composition of the clusters at different concentrations of the added species. The earlier mutual coagulation theory of Hogg *et al.*¹⁴ only treated the coagulation rate between the primary particles, which cannot be used to predict the size, the structure, or the composition of the clusters. Although Hogg *et al.*¹⁴ suggested that at long times heterocoagulation will result in two "phases"—a coagulated "phase" made of the mixture of the two solid components and a disperse "phase" containing only one of the solid components—they could not predict how the size, the composition, or the structure of the mixture "phase" changes with the concentration of the second species particles. To examine the size and composition of the clusters, we used the aggregation model of Shih, Kikuchi, and Aksay,¹⁵ abbreviated as the SKA model. The SKA model was modified from the diffusion-limited-cluster-aggregation (DLCA) model^{16,17} with finite interparticle interactions.¹⁵ The simulations allowed, besides the collisions between the primary particles, the collisions between the clusters as well as the collisions between clusters and particles. It has been shown that the cluster-cluster aggregation mechanism is crucial to the structure and growth rate of the clusters.¹⁶⁻¹⁹ For monodisperse suspensions, the DLCA model has been shown to be representative of colloidal aggregates under irreversible aggregation conditions. With finite interaction energies, the SKA model produced aggregates that are reminiscent of colloidal aggregates under various reversible aggregation conditions.^{15,20} For binary suspensions, the SKA model has been successfully applied to study the depletion flocculation and depletion restabilization phenomena.^{21,22} Therefore, the SKA aggregation model is well suited for studying the heteroflocculation phenomena.⁶⁻¹⁴

II. Model

For convenience, we perform the simulations on a two-dimensional square lattice. Consider a mixture of N_1 first species of particles and N_2 second species of particles placed in a

J. W. Halloran—contributing editor

Manuscript No. 192710. Received April 5, 1995; approved April 3, 1996.
Supported by the Air Force Office of Scientific Research (AFOSR) under Grant No. F49620-93-1-0259; additional support for W.-H. Shih was provided by Drexel University.

^{*}Member, American Ceramic Society.

[†]Princeton University.

[‡]Drexel University.

square lattice of area A . In what follows, we simply refer to the first species of particles as particles 1 and the second species of particles as particles 2. The number density of particles 1 is $c_1 = N_1/A$ and that of particles 2 is $c_2 = N_2/A$. The total particle number density is $c = c_1 + c_2$. We take the area of a unit cell to be unity. Thus, $c = 1$ represents the case where the lattice is fully occupied. An unoccupied site represents the solvent. For simplicity, we only consider nearest-neighbor interactions. The interaction energy between an i th species of particle and its neighboring j th species of particle is denoted as E_{ij} . In other aggregation models such as the DLCA model,^{16,17} the interparticle attraction energy is implicitly infinite; therefore, aggregation is irreversible. In the SKA model, we allow finite interparticle interaction energies so that a broader range of aggregation conditions can be assessed. For binary suspensions, the model was applied to study the depletion–floculation and the depletion–restabilization phenomena.^{21,22} For the present study on heterofloculation, we consider cases where both E_{11} and $E_{22} > 0$ while $E_{12} < 0$; that is, attraction exists only between unlike particles.

Initially, we randomly distribute the N_1 particles 1 and the N_2 particles 2 in an $M \times M$ lattice with periodic boundary conditions. This random distribution is to mimic the initial mixing in the experiments. The particles then perform Brownian motion (random walk). A particle of the i th species moves one lattice constant after every $\tau_{D,i}$. However, the Brownian motion of a particle may be modified when the particle is in the vicinity of other particles because of the interparticle interactions. The modification is incorporated in the simulations by means of a Boltzmann factor and is simulated by the Monte Carlo method.

When two particles are adjacent to each other, they form a cluster and move as a whole. Because of finite attraction energies, a particle within a cluster can break up from its neighbors by thermal motion. A particle of the i th species may attempt to unbind from its neighbors after each time interval $\tau_{R,i}$. The unbinding of a particle from its neighboring particles, leading to the fragmentation of a cluster, is also determined by a Boltzmann factor and simulated by the Monte Carlo method. The details of the simulation procedure are in previous publications.^{17,20,21}

The mobility of a cluster is assumed to be inversely proportional to its mass. Except for this difference, a cluster is treated the same as a particle. That is, clusters also perform Brownian motion and the motion is modified by the Boltzmann factor.

When two clusters collide, they form a larger cluster as well. Very large clusters may appear as motionless within the time frame of the simulations. However, we did not keep track of the cluster mobility in the present study. Further, we did not consider sedimentation due to gravitational effect.

The parameter $\tau_{D,i}$, where $i = 1$ or 2 , is related to the diffusivity of the i th species of particles. The unbinding time constant, $\tau_{R,i}$, is the inverse of the unbinding attempt frequency of the i th species of particles and is related to the surface properties of the particles.^{17,20,21} In general, $\tau_{D,i}$ is different from $\tau_{R,i}$. The mobility of particles 1 can also be different from that of particles 2. Unless mentioned, we use $\tau_{D,i} = \tau_{R,i} = \tau_D$. The choice of a different set of $\tau_{D,i}$ and $\tau_{R,i}$ would mainly affect the aggregation rate but not the qualitative behavior and our choice for $\tau_{D,i}$ and $\tau_{R,i}$ in the present paper is arbitrary. A small $\tau_{D,i}$ may be interpreted as a higher particle mobility and a smaller $\tau_{R,i}$ may be interpreted as a higher relaxation rate.

III. Results

Figures 1(a–c) show how the aggregate size varies with particle-2 concentration for $E_{11} = 5.0$, $E_{12} = 3.0$, $E_{22} = 8.0$, and $c_1 = 0.041$ where the interaction energies are in units of $k_B T$. Figures 1(a–c) are the results of two-dimensional simulations. The simulations were performed in a 35×35 lattice with periodic boundary conditions. The cluster size in Fig. 1(b) is larger than that in either Fig. 1(a) or Fig. 1(c). In the absence of particles 2, particles 1 are stable. Upon the introduction of particles 2 into the suspension of particles 1, heterofloculation occurs between particles 1 and particles 2 as a result of the attractive interaction between particles 1 and particles 2, which leads to an initial increase in cluster size at low particle-2 concentrations. For clarity, we highlighted the largest clusters where the size of the largest cluster increases from Fig. 1(a) to (b). Upon further increase in particle-2 concentration, the coverage of particles 2 on particles 1 becomes higher. As a result of the mutual repulsion between particles 2, the cluster size decreases with further increase in particle-2 concentration. As can be seen from Figs. 1(b) to (c), the size of the largest cluster now decreases. In the present study, we averaged all quantities over 10 independent runs. Our previous simulation studies for binary suspensions under depletion floculation conditions have shown that averaging over 10 independent runs is sufficient for numerical certainty.²¹ Meanwhile, we do not

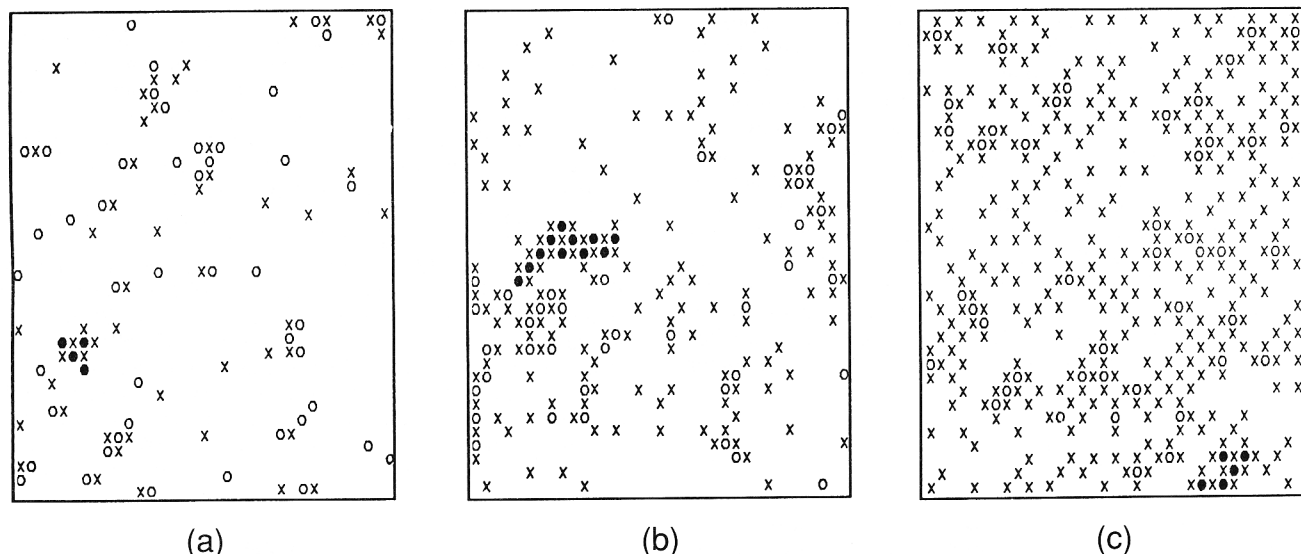


Fig. 1. Snapshot of a binary suspension at $t = 2000\tau_D$ for (a) $c_2 = 0.041$, (b) $c_2 = 0.122$, (c) $c_2 = 0.286$. Open circles represent particles 1 and crosses particles 2. In all three suspensions $c_1 = 0.041$, $E_{11} = 5.0$, $E_{12} = -3.0$, and $E_{22} = 8.0$. The Monte Carlo cell is 35×35 . The largest cluster in each case is highlighted. The cluster size is larger at $c_2 = 0.122$ than at $c_2 = 0.041$ or at $c_2 = 0.286$. Note that clusters consist of both particles 1 and particles 2 under heterofloculation conditions in contrast to clusters formed under depletion floculation conditions that consist of only particles 1 as shown in Figs. 8(a–c).

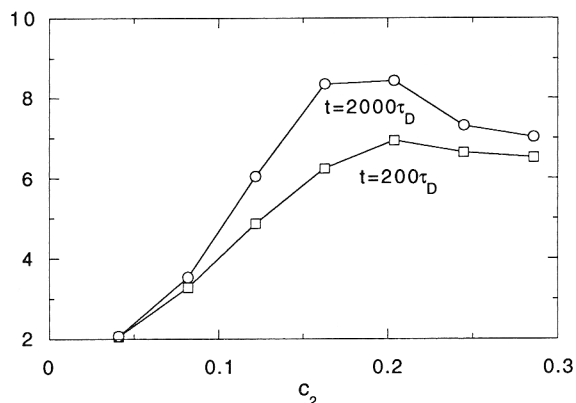


Fig. 2. m versus c_2 at $t = 200\tau_D$ and $t = 2000\tau_D$ where m is the average total number of particles in a cluster regardless of particle types. $c_1 = 0.041$, $E_{11} = 5.0$, $E_{12} = -3.0$, and $E_{22} = 8.0$ as in Fig. 1.

expect the cluster size to change with the size of our Monte Carlo cell since the previous simulations showed no change of cluster size with the system size for binary suspensions.²¹ We designate the average total number of particles in a cluster, regardless of particle type, as m and, in Fig. 2, show its dependence on particle-2 concentration, c_2 at $t = 200\tau_D$ and $t = 2000\tau_D$. Note that m exhibits a peak with respect to c_2 and the cluster size increases with time, especially, near the peak. The time dependence of the cluster size is typical of flocculated suspensions as flocculation is a nonequilibrium phenomenon.^{21,22} In the adsorption studies of hydrated alumina (HA) particles (20 nm in diameter) on silicon nitride (0.7 μm in diameter),⁹ the adsorbed particles were much smaller than silicon nitride particles, and the cluster size observed in the experiment was mainly due to silicon nitride particles. To compare with the experiment,⁹ we also examine m_1 , the average number of particles 1 in a cluster. Figure 3 shows m_1 versus c_2 at $t = 200\tau_D$ and $t = 2000\tau_D$. We see that m_1 also exhibits a maximum with respect to c_2 . As similar to the peak in m , the peak value of m_1 also increases with time. The initial increase in m and m_1 at lower c_2 is due to the bridging of particles 1 by particles 2 as can be seen from Fig. 1(a). The decrease in both m and m_1 at higher concentrations of particles 2 is attributed to the repulsion between particles 2. The repulsion between particles 2 makes the particle-2-covered particles 1 more stable against further flocculation. As m_2 is the average number of particles 2 in a cluster and m_1 is that of particles 1, the ratio m_2/m_1 can be used to represent the number of particles 2 adsorbed on each particle 1. Figure 4 shows m_2/m_1 as a function of c_2 at $t = 200\tau_D$ and $t = 2000\tau_D$ where m_2/m_1 represents the number of

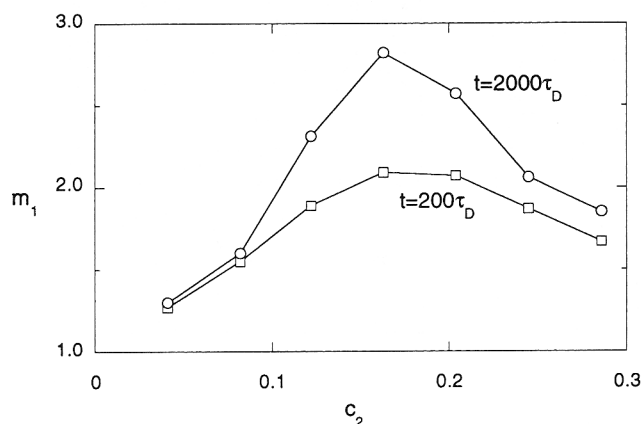


Fig. 3. m_1 versus c_2 at $t = 200\tau_D$ and $t = 2000\tau_D$ where m_1 is the average number of particles 1 in a cluster. $c_1 = 0.041$, $E_{11} = 5.0$, $E_{12} = -3.0$, and $E_{22} = 8.0$ as in Figs. 1 and 2.

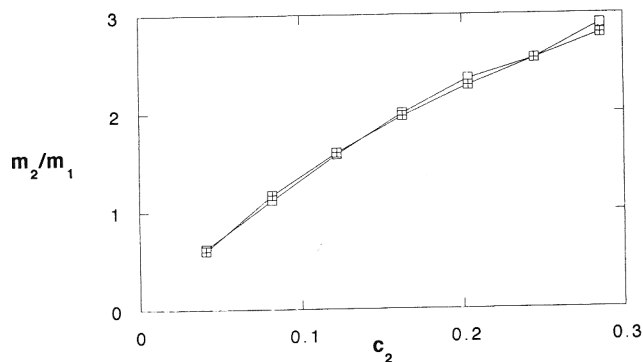


Fig. 4. m_2/m_1 versus c_2 at $t = 200\tau_D$ and $t = 2000\tau_D$ where m_1 is as defined in Fig. 3 and m_2 is the average number of particles 2 in a cluster. The ratio m_2/m_1 can be used to represent the number of particles 2 adsorbed on each particle 1. Although the cluster size grows with time as can be seen from Figs. 2 and 3, the ratio m_2/m_1 does not change much with time.

particles 2 adsorbed per particle 1. In the present model, a ratio of $m_2/m_1 = 4$ represents full adsorption due to the square lattice we have employed and a ratio of $m_2/m_1 = 2-3$ represents a very high adsorption amount that makes further flocculation more difficult. As a result, the cluster size decreases at higher concentrations of particles 2. The observation of a peak in the average cluster size m_1 (or m) with respect to c_2 in the present simulation is similar to the experiment of binary suspensions of small hydrated alumina particles and large Si_3N_4 particles.⁹ In the Si_3N_4 /HA suspensions, the cluster size was shown to exhibit a peak with respect to HA concentration.⁹ Meanwhile, in suspensions that have adsorbing polymers, minima in suspension stability have been observed.^{11,12} The minima in suspension stability are consistent with the maxima in cluster size observed in the present simulations as well as in Si_3N_4 /HA suspensions.⁹ Bridging in particle-polymer suspensions is caused by the adsorption of polymers on the particle surface.^{11,12}

The effect of E_{22} on the location of the peak as well as the height of the peak is shown in Fig. 5 by plotting m_1 versus c_2 at $t = 2000\tau_D$. All parameters except E_{22} are held the same as in Figs. 1-4, i.e., $E_{11} = 5.0$, $E_{22} = 8.0$, and $c_1 = 0.041$. As E_{22} decreases, the peak shifts to a higher c_2 and its peak height also increases. This result agrees with the experimental observation in Si_3N_4 /HA suspensions where the peak in cluster size shifts to a higher HA concentration as the ζ -potential of HA decreases.⁹

The effect of the concentration of particles 1 is shown in Fig. 6, where m_1 is plotted as a function of c_2 for $c_1 = 0.0245$, 0.041, and 0.065 at $t = 2000\tau_D$. Figure 6 shows that as c_1

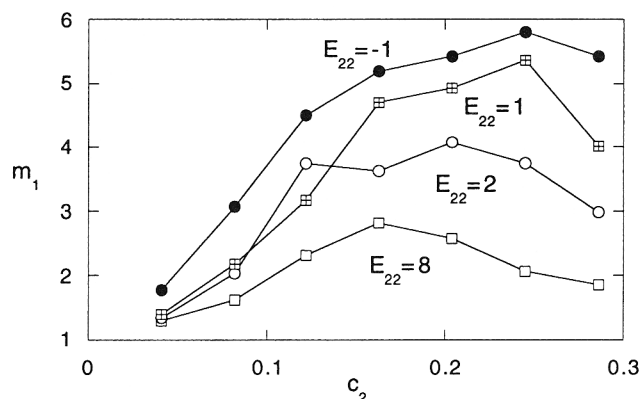


Fig. 5. m_1 versus c_2 at $t = 2000\tau_D$ for $E_{11} = 8.0$ (open squares), $E_{12} = 2.0$ (open circles), $E_{22} = 1.0$ (open squares with crosses), and $E_{22} = -1.0$ (full circles). The rest of the parameters are the same as in Figs. 1-4. As E_{22} decreases, the peak height in m_1 increases and the location of the peak shifts to a higher c_2 .

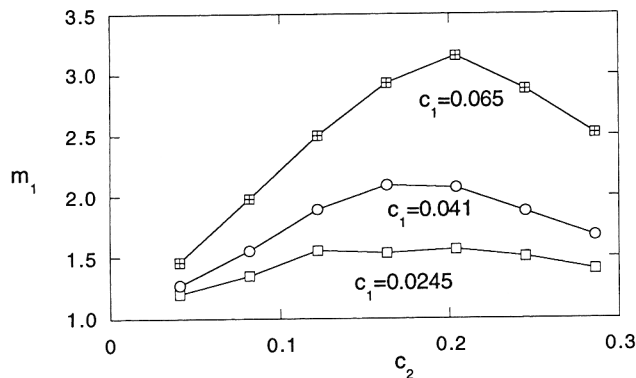


Fig. 6. m_1 versus c_2 at $t = 2000\tau_D$ for $c_1 = 0.0245$ (open squares), $c_1 = 0.041$ (open circles), and $c_1 = 0.065$ (open squares with crosses). The rest of the parameters are the same as in Figs. 1–4. As c_1 increases, the peak height in m_1 increases and the location of the peak shifts to a higher c_2 .

increases, the peak in the cluster size m_1 shifts to a higher c_2 and its height increases. The increase in the peak height as well as the shift of the peak to a higher c_2 at a high c_1 is due to the lower adsorption amount m_2/m_1 as a result of a higher c_1 . As a result, particles as well as clusters are less stable against further flocculation. This can be seen in Fig. 7, where m_2/m_1 is plotted as a function of c_2 for $c_1 = 0.0245$, 0.041 , and 0.065 at $t = 2000\tau_D$. The ratio m_2/m_1 decreases with an increasing c_1 .

IV. Discussion

Although heteroflocculation can cause the cluster size to undergo a maximum with respect to the concentration of the second species of particles as shown in the present work and by others,^{9,11,12} a maximum in cluster size with respect to the concentration of the second species of particles may also arise under depletion flocculation conditions,^{21,22} i.e., $E_{11} < 0$, and E_{12} and $E_{22} > 0$. An example is shown for $E_{11} = -1$, $E_{12} = E_{22} = 3$, and $c_1 = 0.245$ in Figs. 8(a–c), which are snapshots at $100\tau_D$ for (a) $c_2 = 0$, (b) $c_2 = 0.122$, and (c) $c_2 = 0.245$ taken

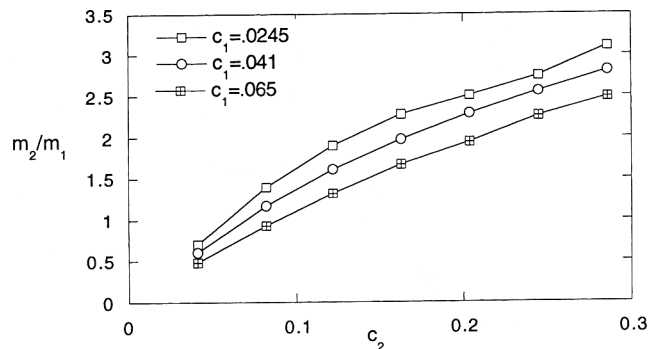


Fig. 7. m_2/m_1 versus c_2 at $t = 2000\tau_D$ for $c_1 = 0.0245$ (open squares), $c_1 = 0.041$ (open circles), and $c_1 = 0.065$ (open squares with crosses). The rest of the parameters are the same as in Figs. 1–4 and 6. At a given c_2 , the ratio m_2/m_1 decreases as c_1 decreases.

from Ref. 21. Note that Figs. 8(a–c) were also the results of two-dimensional simulations as similar to Figs. 1(a–c). Both Figs. 1(a–c) and 8(a–c) were simulated by the same model.²¹ The difference between these two figures results directly from the different interaction energies. The largest clusters are highlighted for clarity. Cluster size undergoes a maximum with respect to c_2 . Under depletion flocculation conditions, the initial increase in cluster size upon the introduction of particles 2 is due to the increase of the effective concentration of particles 1 by the presence of the second species of particles.^{21,22} The decrease in the cluster size at higher particle-2 concentrations is due to the slowing down of particle movement at high particle concentrations.^{21,22} Therefore, the observation of the maxima of the cluster size as well as the viscosity with respect to the concentration of the second species of particles alone cannot distinguish whether clustering in the suspension is caused by depletion flocculation or by heteroflocculation. The key to distinguish the clustering mechanism is to examine the makeup of the clusters. In depletion flocculation, only particles 1 are mutually attractive, i.e., $E_{11} < 0$, and E_{12} and $E_{22} > 0$. Therefore, clusters consist only of particles 1, as can be seen from

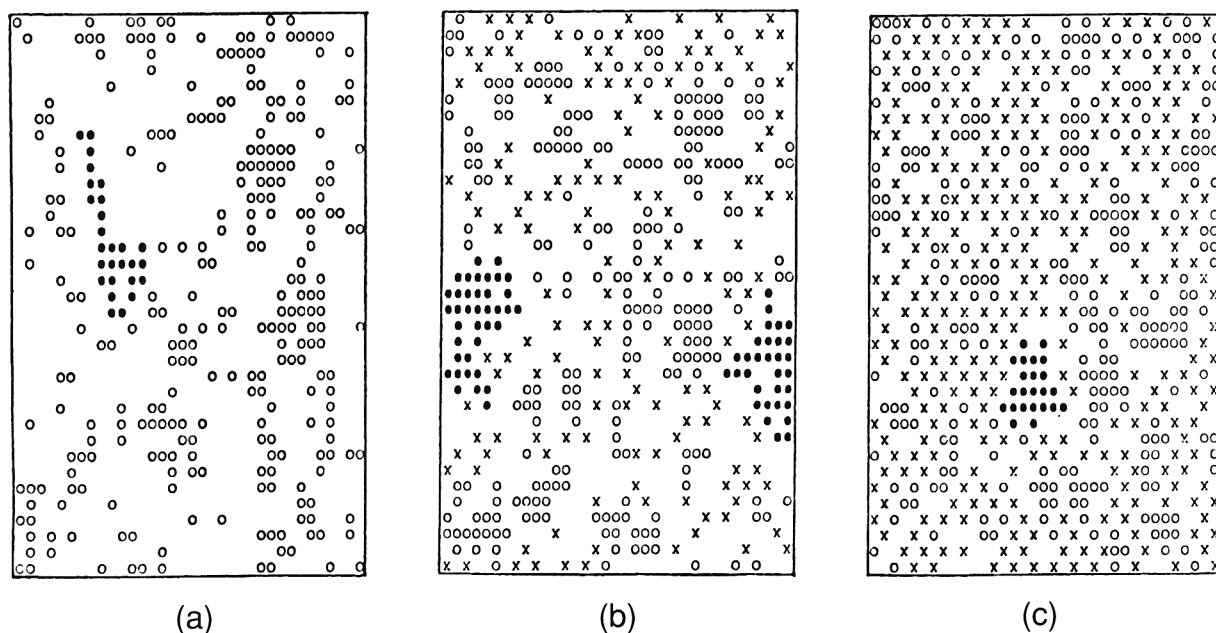


Fig. 8. Snapshot at $100\tau_D$ under depletion flocculation conditions for (a) $c_2 = 0$, (b) $c_2 = 0.122$, and (c) $c_2 = 0.245$, which were the results of two-dimensional simulations taken from Ref. 19. In all cases, $E_{11} = -1$, $E_{12} = E_{22} = 3$, and $c_1 = 0.245$. The open circles represent particles 1 and the crosses particles 2. The largest clusters are highlighted for clarity. Cluster size undergoes a maximum with respect to c_2 . Clusters only consist of particles 1 under depletion conditions in contrast to clusters formed under heteroflocculation conditions that consist of both particles 1 and particles 2 as shown in Figs. 1(a–c).

Figs. 8(a–c), whereas in heteroflocculation, particles 2 are attractive to particles 1, i.e., $E_{12} < 0$, and E_{11} and $E_{22} > 0$. Therefore, clusters consist of both particles 1 and particles 2, as can be seen from Figs. 1(a–c). To examine the makeup of clusters experimentally, we may use transmission electron microscopy or scanning electron microscopy. In principle, we would expect a structure consisting of clusters of particles 1 segregated from patches of particles 2 for depletion flocculation^{21,22} as similar to Figs. 8(b–c) and a micrograph of clusters of intimately mixed particles 1 and particles 2 for heteroflocculation as similar to Figs. 1(a–c). Another way to discern the makeup of the clusters would be to centrifuge the suspension under conditions where the peak in cluster size occurs. In the case of heteroflocculation, adsorption saturates around where the cluster size peaks. Therefore, centrifugation of a suspension undergoing heteroflocculation would leave few particles 2 in the supernatant since most of particles 2 are inside the settling clusters. Under depletion flocculation conditions, clusters do not contain particles 2. Therefore, the supernatant of a suspension that undergoes depletion flocculation would retain most of particles 2. By examining the particle-2 concentration in the supernatant after centrifugation, one may distinguish whether the observed clustering is caused by depletion flocculation or by heteroflocculation. If the particle-2 concentration in the supernatant is much smaller than the initial value, clustering is caused by heteroflocculation. On the other hand, if the particle-2 concentration in the supernatant is not much reduced from the initial particle-2 concentration, clustering is caused by depletion flocculation.

As mentioned above, experimentally, heteroflocculation can be caused either by electrostatic attractions when the two species of particles carry opposite charges^{6–8} or by reduction in the repulsive barrier when the diameter of one of the species of particles is much smaller than that of the other species of particles.⁹ Because of the use of nearest-neighbor interactions, we did not simulate aggregation in the presence of a repulsive barrier. Aggregation in the presence of a repulsive barrier can be simulated if a longer range of interactions is considered. The simplest model for interactions with a repulsive barrier can be obtained if nonzero interaction energies are considered for the second nearest neighbors: A negative first-nearest-neighbor interaction energy represents the primary minimum while a positive second-nearest-neighbor interaction energy represents the barrier.

V. Conclusions

We have performed computer simulations of heteroflocculation in a binary suspension where only particles of different kinds exhibit mutual attractions. The most salient feature of the simulation results is that at a fixed concentration of particles 1 the cluster size exhibits a peak with respect to concentration of particles 2. The decrease in cluster size at a higher concentration of particles 2 is attributed to the repulsion between particles 2. The repulsion between particles 2 makes the particle-2-covered particles 1 more stable against further flocculation. The peak in cluster size as a function of particle-2 concentration shown in the present simulations is similar to recent experiments on binary suspensions of small hydrated alumina particles (20 nm in diameter) and large Si_3N_4 particles (0.7 μm in diameter) where cluster size was shown to exhibit a peak with respect to the hydrated alumina concentration.⁹ The maximum in cluster size is also consistent with minima in suspension stability observed in suspensions where bridging flocculation is caused by polymer adsorption.^{11,12} The peak height in cluster

size increases and the peak shift to a higher particle-2 concentration as the repulsion between particles 2 decreases. This is consistent with the fact that repulsion between particles 2 causes the decrease in cluster size at higher particle-2 concentrations. The increase of the peak height as well as the shift of the peak to a higher c_2 with a decreasing E_{22} agrees with the experimental observations that the peak in cluster size shifts to a higher HA concentration as the ζ -potential of HA decreases.⁹ In addition, we also showed that as the concentration of particles 1 increases, the peak height in the cluster size increases and the peak shifts to a higher concentration of particles 2. The increase in the cluster size as well as the shift of the peak to a higher concentration of particles 2 is attributed to the lower adsorption amount of particles 2 on particles 1 at a higher concentration of particles 1. To maximize packing density, under the conditions of present simulations, the concentration range of particles 2 where the maximum of cluster size occurs should be avoided.

References

1. A. Aksay, D. M. Dabbs, and M. Sarikaya, "Mullite for Structural, Electronic, and Optical Applications," *J. Am. Ceram. Soc.*, **74** [10] 2343–58 (1991), and the references cited therein.
2. C.-L. Hu and M. N. Rahaman, "Factors Controlling the Sintering of Ceramic Particulate Composites: II, Coated Inclusion Particles," *J. Am. Ceram. Soc.*, **75** [8] 2066 (1992).
3. T.-I. Mah, K. S. Mazdhyasni, and R. Ruh, "Characterization and Properties of Hot-Pressed Si_3N_4 with Alkoxy-Derived CeO_2 and Y_2O_3 as Sintering Aids," *J. Am. Ceram. Soc.*, **58** [9] 88 (1979).
4. T. M. Shaw and R. A. Pethica, "Preparation and Sintering of Homogeneous Silicon Nitride Green Compacts," *J. Am. Ceram. Soc.*, **69** [2] 88 (1986).
5. W.-H. Shih, L.-L. Pwu, and A. A. Tseng, "Boehmite Coating as a Consolidation and Forming Aid in Aqueous Silicon Nitride Processing," *J. Am. Ceram. Soc.*, **78** [5] 1252–60 (1995).
6. E. Liden, M. Persson, E. Carlstrom, and R. Carlsson, "Electrostatic Adsorption of a Colloidal Sintering Agent on Silicon Nitride Particles," *J. Am. Ceram. Soc.*, **74** [6] 1335 (1991).
7. P. E. Debely, E. A. Barringer, and H. K. Bowen, "Preparation and Sintering Behavior of Fine-Grained Al_2O_3 - SiO_2 Composites," *J. Am. Ceram. Soc.*, **68** [3] C-76–C-78 (1985).
8. T. Garino, "Heterocoagulation as an Inclusion Coating Technique for Ceramic Composite Processing," *J. Am. Ceram. Soc.*, **75** [3] 514–18 (1992).
9. W.-H. Shih, D. Kisailus, W. Y. Shih, Y.-H. Hu, and J. Hughes, "Rheology and Consolidation of Colloidal Alumina-Coated Silicon Nitride Suspensions," *J. Am. Ceram. Soc.*, **79** [5] 1155–62 (1996).
10. E. Dickenson, "A Model of a Concentrated Dispersion Exhibiting Bridging Flocculation and Depletion Flocculation," *J. Colloid Interface Sci.*, **132** [1] 274–78 (1989).
11. S. G. Ash and E. J. Clayfield, "Effect of Polymers on the Stability of Colloids: Flocculation of Polystyrene Latex by Polyethers," *J. Colloid Interface Sci.*, **55** [3] 645–57 (1976).
12. C. Cowell and B. Vincent, "Flocculation Kinetics and Equilibria in Sterically Stabilized Dispersions," *J. Colloid Interface Sci.*, **95** [2] 573–82 (1983).
13. L. H. Princen and M. DeVena-Peplinski, "Effect of Particle Size on the Mutual Flocculation between Zinc Oxide and Titanium Dioxide," *J. Colloid Sci.*, **19**, 786–97 (1964).
14. R. Hogg, T. W. Healy, and D. W. Fuerstenau, "Mutual Coagulation of Colloidal Dispersions," *Trans. Faraday Soc.*, **62**, 1630–51 (1965).
15. W. Y. Shih, R. Kikuchi, and I. A. Aksay, "Reversible-Growth Model: Cluster-Cluster Aggregation Model with Finite Binding Energies," *Phys. Rev. A*, **36**, 5015–19 (1987).
16. P. Meakin, "Formation of Fractal Clusters and Networks by Irreversible Diffusion-Limited Aggregation," *Phys. Rev. Lett.*, **51**, 1119 (1983).
17. M. Kolb, R. Botet, and R. Jullien, "Scaling of Kinetically Growing Clusters," *Phys. Rev. Lett.*, **51**, 1123 (1983).
18. D. A. Weitz and M. Olivera, "Fractal Structures by Kinetic Aggregation of Aqueous Gold Colloids," *Phys. Rev. Lett.*, **52**, 1433 (1984).
19. C. Aubert and D. S. Cannell, "Restructuring of Colloidal Silica Aggregates," *Phys. Rev. Lett.*, **56**, 738 (1986).
20. W. Y. Shih, J. Liu, W.-H. Shih, and I. A. Aksay, "Aggregation of Colloidal Particles with a Finite Interparticle Attraction Energy," *J. Stat. Phys.*, **62**, 961 (1991).
21. J. Liu, W. Y. Shih, R. Kikuchi, and I. A. Aksay, "Clustering of Binary Colloidal Suspensions: Theory," *J. Colloid Interface Sci.*, **142**, 369 (1991).
22. M. Yasrebi, W. Y. Shih, and I. A. Aksay, "Clustering of Binary Colloidal Suspensions: Experiment," *J. Colloid Interface Sci.*, **142**, 357 (1991), and the references cited therein. □